

See discussions, stats, and author profiles for this publication at: <https://www.researchgate.net/publication/243656041>

# Vibrational spectra and force constants of heptasulfur imide S<sub>7</sub>NH

ARTICLE *in* THE JOURNAL OF PHYSICAL CHEMISTRY · FEBRUARY 1977

Impact Factor: 2.78 · DOI: 10.1021/j100519a013

---

CITATIONS

23

---

READS

7

1 AUTHOR:



Ralf Steudel

Technische Universität Berlin

357 PUBLICATIONS 4,655 CITATIONS

SEE PROFILE

# Vibrational Spectra and Force Constants of Heptasulfur Imide

Ralf Steudel

*Institut für Anorganische und Analytische Chemie, Technische Universität Berlin, Berlin-Charlottenburg, West Germany (Received August 20, 1976)*

*Publication costs assisted by Verband der Chemischen Industrie*

Raman, infrared, and far-infrared spectra of solid and dissolved  $S_7NH$ ,  $S_7ND$ ,  $S_7^{15}NH$ , and  $S_7^{15}ND$  have been recorded. All fundamental frequencies of heptasulfur imide have been observed and assigned in accordance with the molecular symmetry  $C_s$ . A normal-coordinate treatment was carried out using a modified Urey-Bradley force field with 16 independent force constants. Good agreement between observed and calculated frequencies was obtained and both Urey-Bradley and valence force constants are reported.

## Introduction

In recent years the vibrational spectra of certain sulfur rings such as  $S_6$ ,<sup>1</sup>  $S_8$ ,<sup>2</sup> and  $S_{12}$ <sup>3</sup> have been definitely assigned. These rings belong to the degenerate point groups  $D_{3d}$  and  $D_{4d}$ , respectively, and since there are no substituents the spectra consist of relatively few absorptions and Raman lines, respectively. It has been shown that the spectra can be understood by means of very simple Urey-Bradley force fields with six or seven independent force constants only. For these reasons sulfur rings are ideal molecules to study the dependence of certain fundamental vibrations on ring size and molecular symmetry as well as possible relationships between force constants and structural parameters.<sup>4,5</sup>

Oxidation of  $S_8$  with trifluoroperacetic acid yields  $S_8O$ <sup>6</sup> whose molecules still contain eight-membered puckered rings but with  $C_s$  symmetry.<sup>7</sup> The oxygen is linked to one of the sulfur atoms by a double bond in an axial position. The vibrational spectra of  $S_8O$  have been investigated<sup>8</sup> and force constants have been calculated.<sup>9</sup> The results show that the lowering of ring symmetry in  $S_8O$  compared with  $S_8$  causes all bending and torsional modes degenerate in  $S_8$  to split into their components but without much change in average frequency and Raman intensity.<sup>9</sup>

Another possibility to lower the symmetry of the  $S_8$  ring is substitution of one sulfur atom by a heteroatom. The simplest compound of this type whose structure is known and which can be prepared in high purity is heptasulfur imide,  $S_7NH$ .  $S_7NH$  forms almost colorless crystals which can be prepared, for example, from  $S_8$  by treatment with  $NaN_3$  in tris(dimethylamino)phosphine oxide, subsequent hydrolysis in aqueous hydrochloric acid, and purification of the crude product by repeated recrystallization or column chromatography.<sup>10</sup> The molecular structure of  $S_7NH$  has been investigated several times<sup>11,12</sup> but only recently was it possible to determine the positions of all atoms including the hydrogen by x-ray diffraction on single crystals at  $-160^\circ C$ .<sup>13</sup> The molecules consist of crown-shaped  $S_7N$  rings containing almost planar groups  $S_2NH$ . The molecular and site symmetry is  $C_s$  and the centrosymmetric unit cell contains four molecules. The geometrical parameters are given in Table I; the numbering of atoms and bonds is shown in Figure 1.

The vibrational spectra of  $S_7NH$  were first investigated by Nelson<sup>14</sup> who recorded the Raman spectrum in the region  $40\text{--}3500\text{ cm}^{-1}$  and the infrared spectrum in the region  $200\text{--}4000\text{ cm}^{-1}$  using solid  $S_7NH$  and solutions in  $CS_2$ . However, Nelson did not observe all fundamental frequencies and made only a few assignments. Furthermore, some of the wavenumbers given in Tables 2 and 3 of Nelson's paper do not agree with the values which can

TABLE I: Bond Distances ( $r$ , Å), Valence Angles ( $\alpha$ ,  $\beta$ , deg), and Dihedral Angles ( $\tau$ , deg) of Heptasulfur Imide<sup>a</sup>

$r_1, r_2$	2.048	$\alpha_1$	107.2	$\tau_1, \tau_2$	93.5
$r_3, r_4$	2.062	$\alpha_2, \alpha_3$	106.8	$\tau_3, \tau_4$	99.4
$r_5, r_6$	2.049	$\alpha_4, \alpha_5$	108.3	$\tau_5, \tau_6$	94.8
$r_7, r_8$	1.676	$\alpha_6, \alpha_7$	110.1	$\tau_7, \tau_8$	96.5
$R_9$	0.91	$\alpha_8$	123.8	$\beta_1, \beta_2$	117.1

<sup>a</sup> The angle at atom  $i$  is termed  $\alpha_i$ , the two angles  $SNH$  are termed  $\beta_1$  and  $\beta_2$ , and the torsion angle at the bond  $r_i$  is called  $\tau_i$ .

be obtained from her Figures 2a and 2b.

To remove these discrepancies and to determine all fundamental frequencies of the heptasulfur imide molecule we recorded the Raman, infrared, and far-infrared spectra of  $S_7NH$ ,  $S_7ND$ ,  $S_7^{15}NH$ , and  $S_7^{15}ND$  in the solid state as well as in  $CS_2$  solutions and made a normal-coordinate analysis.

## Experimental Section

$S_7NH$  was prepared from  $S_8$  and  $NaN_3$ <sup>10</sup> since this method yields only traces of  $S_6(NH)_2$  and  $S_5(NH)_3$  which can be separated from  $S_7NH$  by chromatography only.<sup>15</sup> The crude product was extracted with boiling methanol from which on cooling  $S_8$  crystallizes first followed by  $S_7NH$  on evaporation. The samples used for spectroscopy were purified by repeated recrystallization from  $CH_3OH$  and  $CCl_4$  and in some cases by chromatography and showed melting points between  $109$  and  $113^\circ C$ . All samples were free of  $S_6(NH)_2$  as checked by thin-layer chromatography. Only traces of  $S_8$  were present in some cases but since all strong IR absorptions and Raman lines, respectively, of  $S_7NH$  no differences in the spectra of samples from different preparations were observed.

Since the hydrogen in  $S_7NH$  is fairly acidic ( $pK_a = 5^{16}$ )  $S_7ND$  was easily obtained by recrystallization of  $S_7NH$  from excess methanol- $d_1$  ( $\geq 99$  atom %  $CH_3OD$ ) or alternatively by very slow precipitation of 2 g of  $S_7NH$  dissolved in 120 ml of dry acetone with 50 ml of  $D_2O$  ( $\geq 99.7$  atom %  $D_2O$ ) and subsequent drying under high vacuum for several hours.

On standing in air  $S_7ND$  changes to  $S_7NH$  within 24 h. Therefore, due to the conventional sample preparation the IR spectra of  $S_7ND$  exhibited additional weak absorptions belonging to  $S_7NH$ .

$S_7^{15}NH$  was prepared from  $K^{15}NN_2$  (95 atom %  $^{15}N$  at one terminal atom of the azide anion) which first had to be converted into  $Na^{15}NN_2$  by ion exchange since  $KN_3$  does not react with  $S_8$  to give  $S_7NH$  in good yields. 1.6 g of  $Na^{15}NN_2$  was stirred with 1.7 g of  $S_8$  in 33 ml of

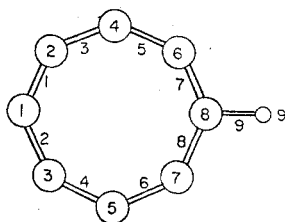


Figure 1. Numbering of atoms and bonds in heptasulfur imide.

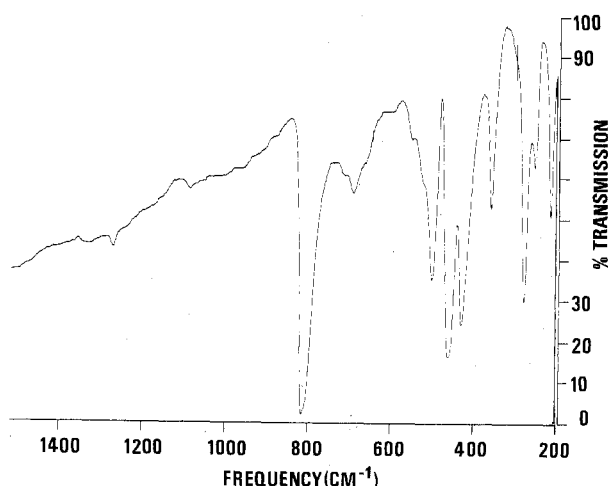


Figure 2. Infrared spectrum of solid  $S_7NH$  at 25 °C.

$[(CH_3)_2N]_3PO$ , the reaction bottle being placed in a nitrogen filled desiccator over  $CaCl_2$ . After hydrolysis in 40 ml of 10% hydrochloric acid and drying under high vacuum the crude product was extracted with 140 ml of hot methanol for 1 hr. After cooling and filtration the solvent was evaporated and the residue dissolved in  $CS_2$ . This solution was used for column chromatography on silica gel eluting with a mixture of equal volumes of  $CCl_4$  and  $n$ -hexane. The presence of  $S_7NH$  in the eluate was checked with alcoholic potassium hydroxide (turns violet with  $S_7NH$ ). After evaporation of the medium fraction and drying under high vacuum colorless crystals of a  $S_7^{14}NH/S_7^{15}NH$  mixture (1:1) were obtained (melting point 113 °C). In the following this mixture is denoted  $S_7^*NH$ . All chemicals used were of the highest commercially available quality.

The Raman spectra were recorded in the region 10–3500  $cm^{-1}$  using a Cary 82 spectrometer with triple monochromator and the 488.0-, 514.5-, and 647.1-nm lines of Ar and Kr lasers. Powdered samples as well as solutions in  $CS_2$  (freshly distilled from  $P_4O_{10}$ ) were investigated. With Ar laser excitation a rotating sample holder was used for solid samples. Polarization measurements were possible for the strongest Raman lines only since the solubility is not very high.

The infrared spectra in the region 200–4000  $cm^{-1}$  were recorded using two grating spectrometers (Beckman IR 12 and Perkin-Elmer 325). KBr, CsBr, and CsI disks were prepared with 5–35 mg of heptasulfur imide. Low temperature spectra were recorded using a device described earlier.<sup>17</sup> Solutions in  $CS_2$  were investigated in matched 0.1–1.0-mm cells of CsI. The region 50–400  $cm^{-1}$  was also investigated with a Polytec FIR 30 Fourier transform spectrometer using sample disks prepared from pure  $S_7NH$ .

### Vibrational Spectra and Frequency Assignment

The observed infrared bands and Raman lines are listed in Tables II–IV and the spectra are shown in Figures 2–4. For a molecule of  $C_s$  symmetry consisting of 9 atoms, 21

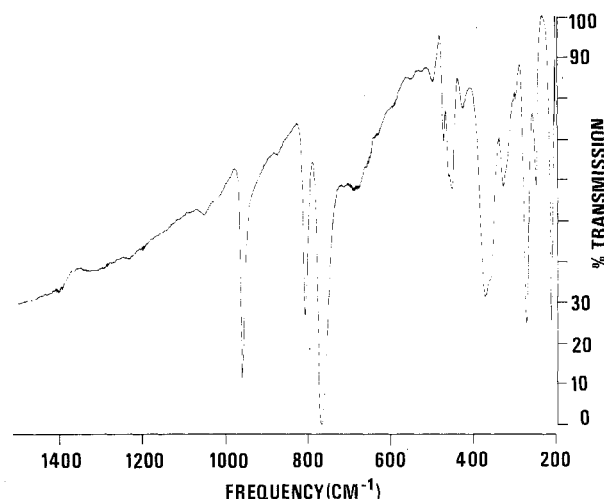


Figure 3. Infrared spectrum of solid  $S_7ND$  at 25 °C (containing approximately 10%  $S_7NH$ ).

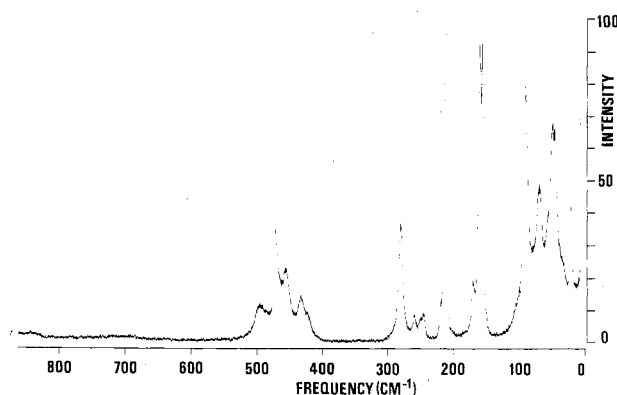


Figure 4. Raman spectrum of solid  $S_7NH$  at 25 °C (spectral bandwidth 1.5  $cm^{-1}$ ).

fundamental vibrations are to be expected, 12 of which belong to the species  $a'$  and 9 to  $a''$  and all of which are infrared and Raman active. There must be 9 stretching, 10 bending, and 2 torsion vibrations (cf.  $S_8O^9$ ). The NH stretching wavenumber of  $S_7NH$  at 3334  $cm^{-1}$  in  $CS_2$  shifts to 3270  $cm^{-1}$  in the solid due to weak intermolecular  $H\cdots S$  hydrogen bonding.<sup>13</sup> In  $S_7ND$  it occurs at 2475  $cm^{-1}$  corresponding to a H/D ratio of 1.35.  $S_7^*NH$  shows  $\nu_{NH}$  at 3331  $cm^{-1}$  (in  $CS_2$ ) but no splitting was observed which, according to the mass difference between  $^{14}N$  and  $^{15}N$ , should amount to 7  $cm^{-1}$ .

The SN stretching wavenumbers can be expected in the region 600–1000  $cm^{-1}$  since the planar  $HNS_2$  group can be compared with the molecules  $OCls_2$  (673, 634<sup>18</sup>),  $H^{11}Bcls_2$  (892, 740<sup>19</sup>), and  $HNcls_2$  (687, 666<sup>20</sup>) whose  $XCl$  stretching wavenumbers are given in parentheses. The antisymmetric SN vibration is of high IR intensity but does not show up in the Raman spectrum. It shifts on deuteration much more than on  $^{15}N$  substitution because of some coupling with  $\delta_{ND}(a'')$  in  $S_7ND$ . This mode occurs at 1288  $cm^{-1}$  in  $S_7NH$  and at 970  $cm^{-1}$  in  $S_7ND$ . The coupling also causes a substantial increase in IR intensity of  $\delta_{ND}$ . In  $HNcls_2$  the corresponding vibration occurs at 1295  $cm^{-1}$ .<sup>20</sup> The symmetric SN vibration of  $S_7NH$  does also not occur in the Raman spectrum and is of very low IR intensity at 25 °C but can be easily detected in IR spectra taken at –185 °C. The wavenumbers are listed in Table IV.

The six SS stretching wavenumbers ( $3a'$ ,  $3a''$ ) can be expected in the region 400–500  $cm^{-1}$  since there is a linear relationship between SS bond distances and average SS frequency<sup>5</sup> from which  $\nu_{SS} = 458 \text{ } cm^{-1}$  is obtained. Since

TABLE II: Vibrational Wavenumbers of  $S_7NH$  ( $cm^{-1}$ )<sup>a</sup>

Raman		Infrared		Assignment
Solid	In $CS_2$	Solid	In $CS_2$	
21 m				} Lattice
47 } vs				
50 }				
56 w,sh		52 vw		
71 s	obsc	63 w		$a' \tau$
91 vs	89 s	75 w		$a'' \tau$
105 w,sh		96 vw		$91 + 21$ or $63 + 52$
158 vs }	160 vs,dp	107 m		$a' + a'' \delta_{SSS}$
162 vs }		168 m		
171 w	170 vw,sh			2·91
		212 s	204 s	$a'' \delta_{SSS}$
215 vvs	212 vvs,p		211 m	$a' \delta_{SSS}$
220 vw,sh				$160 + 71$
247 w	249 w	250 m	249 m	$a' \delta_{SSS}$
251 vw				$160 + 91$
261 w		260 w		$a'' \delta_{SSN}$
282 s	272 m,p	276 s	272 m	$a' \delta_{SNS}$
		295 w		$212 + 91$
		356 m	358 w-m	$a' \delta_{SSN}$
424 w,sh		427 s	424 s	$a'' \nu_{SS}$
433 m	440 m			$a' \nu_{SS}$
456 m	460 w	456 s	446 s	$a'' \nu_{SS}$
			467 w,sh	$a' \nu_{SS}$
				$a'' \nu_{SS}$
473 s	478 m			$a' \nu_{SS}$
496 m	487 m	500 m	494 m	$a' \nu_{SS}$
		522 w,sh	517 w,sh	$272 + 249$
		552 vw		$500 + 52$ or $500 + 63$
		660 vw,sh		$500 + 160$ or $456 + 212$
		694 w	680 w	$a' \nu_{SN}$
		718 vw		$456 + 261$ or $2 \cdot 356$
		740 vw		$456 + 279$
		816 vvs	805.8 s	$a'' \nu_{SN}$
		1274 vw	1288 m	$a'' \delta_{SNH}$
		3270 m	3334 m	$a' \nu_{NH}$
3258 m-s				

<sup>a</sup> v, very; s, strong; m, medium; w, weak; sh, shoulder; b, broad; p, polarized; dp, depolarized; obsc, obscured by  $CS_2$ ;  $\nu$ , stretching;  $\delta$ , bending;  $\tau$ , torsion vibration.

the bond distances vary by only 0.014 Å, vibrational coupling only causes the  $\nu_{SS}$  to be spread over a certain region. The spectra of  $S_7NH$  and  $S_7ND$  show considerable differences in the 400–500- $cm^{-1}$  region. In the case of  $S_7ND$  five frequencies of low or medium intensity are found in the IR and Raman spectra and can be assigned to the six SS stretching fundamentals assuming one incidental degeneracy at 463  $cm^{-1}$ . Since all the calculations show the SS stretching modes distributed in alternating order to the two symmetry species ( $a' > a'' \approx a' > a'' > a' > a''$ ) we assign the wavenumbers in the 420–480- $cm^{-1}$  region accordingly.

$S_7NH$  exhibits only three strong IR absorptions in the 400–500- $cm^{-1}$  region. These are absent not only in  $S_7ND$  but also in the spectrum of  $(S_7N)_2$ <sup>21</sup> in which two  $S_7N$  rings are connected by a sulfur atom. The same holds for  $S_7NCH_3$ .<sup>22</sup> Therefore, we assume that the wavenumbers at 427, 456, and 498  $cm^{-1}$  in the spectra of  $S_7NH$  are connected with the symmetric NH bending vibration (NH wagging). In  $S_7ND$  this mode occurs as a broad structured absorption at 367  $cm^{-1}$ . In  $S_7NH$  it must be coupled to some extent with the SS stretching modes and we assign the 500- $cm^{-1}$  frequency which occurs in the Raman spectrum at 496  $cm^{-1}$  and is polarized to the highest SS stretching mode which is intensified and shifted from 474  $cm^{-1}$  in  $S_7ND$  by mixing with  $\delta_{NH}(a')$ . This assumption is supported by the normal-coordinate analysis (see below). The two remaining wavenumbers at 456 and 427  $cm^{-1}$  are assigned to  $\delta_{NH}(a')$  assuming a splitting caused by a slightly asymmetric double minimum potential (DMP) as has been observed for NH stretching frequencies previously.<sup>23</sup> The

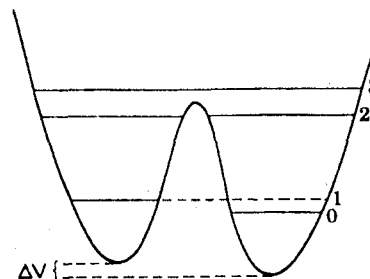


Figure 5. Assumed double minimum potential for the NH wagging mode of heptasulfur imide.

x-ray structure analysis of  $S_7NH$  showed the hydrogen in an axial position with respect to the  $S_7N$  ring but the angle between the NH bond and the plane formed by the neighboring atoms 6, 7, and 8 (see Figure 1) amounts to only 14° (in  $NH_3$ , 56°). Since there must be another position for the hydrogen on the other side of that plane (equatorial position) differing in energy only slightly (due to the different long range SH interaction with atoms 4 and 5) the assumption of a DMP for the wagging vibration seems reasonable. The barrier between the axial and equatorial positions should be quite low causing the first vibrationally excited  $\delta_{NH}$  level to be located near the top of the barrier which results in a splitting of this level (see Figure 5). In this case the relative IR intensities of the transitions 0–2 and 0–3 can be of comparable magnitude.<sup>24,25</sup> On deuteration the levels 0 to 3 decrease in energy and the splitting of levels 2 and 3 becomes much smaller leading to one broad but structured absorption

TABLE III: Vibrational Wavenumbers of  $S_7ND$  ( $cm^{-1}$ )<sup>a</sup>

Raman solid	Infrared		Assignment
	Solid	In $CS_2$	
22 m			} Lattice
46 m			
49 m			
56 w,sh			
70 m			
91 s			$a' \tau$
105 vw,sh			$a'' \tau$
157 } vs			91 + 22
161 }			$a' + a'' \delta_{SSS}$
171 w			2:91
	211 vs	203 vs	$a' \delta_{SSS}$
214 vs		210 m	$a' \delta_{SSS}$
221 w			160 + 70
247 w	247 m	248 s	$a' \delta_{SSS}$
252 w			160 + 91
262 w	262 w		$a'' \delta_{SSN}$
281 m	272 vs	270 s	$a' \delta_{SNS}$
	327 m	312 vs	$a' \delta_{SSN}$
	367 vs,b	368 vs	$a' \gamma_{ND}$
	426 w	427 m	$a'' \nu_{SS}$
439 w	435 vw		$a' \nu_{SS}$
	455 s	461 m	$a'' \nu_{SS}$
460 w,b	464 m	469 m	$a' + a'' \nu_{SS}$
472 s	475 m	478 m	$a' \nu_{SS}$
	501 w		$S_7NH$
		517 w	270 + 248
	658 w	655 w	461 + 204
	680 w-m	676 vw	$a' \nu_{SN}$
		697 w	427 + 270
709 vv			455 + 272
715 vv			
721 vv	723 w	713 w	
729 vv			
	776 vvs	774.5 vvs	$a'' \nu_{SN}$
	966 vs	970 vs	$a'' \delta_{SND}$
	1055 vw,b	1050 vw	970 + 91 or 776 + 272
2425 w	2433 s	2475 s	$a' \nu_{ND}$

<sup>a</sup> For abbreviations see Table II.TABLE IV:  $SN$  Stretching Wavenumbers of Heptasulfur Imide ( $cm^{-1}$ )

Species	State	$S_7^{14}NH$	$S_7^{14}ND$	$S_7^{15}NH$	$S_7^{15}ND$
$a'$	Solid	694	680		
$a''$	In $CS_2$	805.8	774.5	787.0	762.0

band for  $\delta_{ND}(a')$ . This explanation for the strong IR absorptions of  $S_7NH$  in the region 400–500  $cm^{-1}$  is supported by the observation that these bands are observed in  $CS_2$  solution too but shifted to lower wavenumbers due to the cleavage of the weak hydrogen bonds in solid  $S_7NH$ . Furthermore,  $S_7NH$  reacts with tris(dimethylamino)-phosphorus oxide (TDPO) to form the solid adduct TDPO-2 $S_7NH$  in which according to a x-ray structure analysis the two NH groups are hydrogen bonded to the oxygen atom.<sup>26</sup> In this compound  $\delta_{NH}(a')$  occurs at 671  $cm^{-1}$  and  $\delta_{ND}(a')$  at 545  $cm^{-1}$  which in both cases corresponds to a shift from  $S_7NH(D)$  by a factor of 1.5 provided  $\delta_{NH}(a')$  is located near 450  $cm^{-1}$  in  $S_7NH$ .

The assignment of the 10 ring bending and torsional modes is more difficult. The highest frequency at 356  $cm^{-1}$  can be assigned to the symmetric SSN bending mode which according to the lower mass of nitrogen must be the highest ring bending mode.<sup>27</sup> No  $^{14}N/^{15}N$  splitting has been observed for this mode which due to the calculations should amount to 6  $cm^{-1}$ . In  $S_7ND$   $\delta_{SSN}(a')$  is repelled by  $\delta_{ND}(a')$  and therefore shifted to 327  $cm^{-1}$ .

The remaining nine modes can be expected between 300 and 60  $cm^{-1}$  since all corresponding vibrations of  $S_8$  and  $S_8O$  are found in this region. The two torsional modes degenerate in  $S_8$  (85  $cm^{-1}$ ) and split in  $S_8O$  (84, 67  $cm^{-1}$ )

TABLE V: Comparison of Bending and Torsional Modes of Eight-Membered Rings (Symmetry Species, Wavenumbers, Raman Intensities)

$S_8O$ ( $C_8$ )		$S_8$ ( $D_{4d}$ )		$S_7NH$ ( $C_8$ )	
$a'$	219 vs	$a_1$	216 s	$a'$	215 vvs
$a'$	250 vw	$b_2$	243 w	$a'$	282 s
$a'$	190 w			$a'$	356 -
$a''$	197 w	$e_1$	184 w	$a''$	212 obs
$a'$	67 s			$a'$	71 s
$a''$	84 s	$e_2$	85 s	$a''$	91 vs
$a'$	140 s			$a'$	160 } vs
$a''$	157 vs	$e_2$	152 s	$a''$	160 }
$a'$	(219)			$a'$	250 vw
$a''$	235 vw	$e_3$	243 w	$a''$	261 w

can be expected to be of strong Raman intensity and should be located near 80  $cm^{-1}$ . We assign the strong Raman lines at 91 and 70  $cm^{-1}$  to these modes and consider all wavenumbers below 70  $cm^{-1}$  to be lattice modes. In contrast to the 91- $cm^{-1}$  line the 70- $cm^{-1}$  Raman line has not been observed for TDPO-2 $S_7NH$ <sup>26</sup> and  $(S_7N)_2SO$ .<sup>29</sup> However, in  $S_7NH$  and  $S_7ND$   $\tau(a')$  is strongly coupled with  $\delta_{NH(D)}$  which may remove the incidental degeneracy of  $\tau(a')$  and  $\tau(a'')$  which must be assumed for the two derivatives. The lattice vibrations of  $S_8$  have been found below 65  $cm^{-1}$  and some of them give rise to strong Raman lines.<sup>30,31</sup> In  $S_8O$  the lattice vibrations also occur below 65  $cm^{-1}$ .<sup>9</sup> Since  $S_7NH$  is of similar shape and mass as  $S_8$  and  $S_8O$  the wavenumbers of the lattice vibrations should be similar too. Since the unit cell of heptasulfur imide is centrosymmetrical ( $D_{2h}^{16}$ )<sup>11-13</sup> the lattice vibrations may be either Raman or infrared active.

For the assignment of the remaining fundamentals it must be taken into account that only frequencies occurring in all compounds containing the  $S_7N$  unit can be ring bending modes of  $S_7NH$ . Since this is not the case for the Raman lines at 171, 220, and 251  $cm^{-1}$  these frequencies must represent combination vibrations or overtones. The remaining wavenumbers are assigned according to their IR intensities and by analogy with  $S_8$  and  $S_8O$ . The strong Raman line at 160  $cm^{-1}$  slightly split in solid heptasulfur imide has been observed for  $S_8$  at 152  $cm^{-1}$  and for  $S_8O$  at 140/157  $cm^{-1}$  and must represent two modes  $\delta_{SSS}(a' + a'')$  since there is no second line of similar intensity nearby. The splitting in the solid state may arise from correlation field interaction since it is not observed for solid TDPO-2 $S_7NH$ .<sup>26</sup>

The strongest Raman line of  $S_7NH$  occurs at 215  $cm^{-1}$ . This wavenumber is characteristic for eight-membered sulfur rings since it has been observed with high Raman intensity for  $S_8$  (216) and  $S_8O$  (219) also but not for  $S_6$ ,  $S_7$ , and  $S_{12}$ .<sup>4</sup> In the IR spectrum of dissolved  $S_7NH$  two bands occur at 204 and 211  $cm^{-1}$  which correspond to the IR absorption of solid  $S_7NH$  at 212  $cm^{-1}$  and the Raman line at 215  $cm^{-1}$  and represent two SSS bending modes ( $a'' + a'$ ).

The three bending modes left are assigned to the IR absorptions at 276( $a'$ ), 260( $a''$ ), and 250( $a'$ )  $cm^{-1}$ . The 276- $cm^{-1}$  frequency must be the SNS bending mode because of its high IR intensity and its shift on isotopic substitution (in  $CS_2$ :  $S_7NH$  272,  $S_7ND$  270,  $S_7^*NH$  270,  $S_7^*ND$  268  $cm^{-1}$ ).

In Table V the ring bending and torsional modes of  $S_8$ ,  $S_8O$ , and  $S_7NH$  are compared. No differences in the spectra of  $S_7NH$ ,  $S_7ND$ ,  $S_7^*NH$ , and  $S_7^*ND$  were observed below 260  $cm^{-1}$ .

## Force Field

The force constant calculations were made using a modified Urey-Bradley force field since this field was shown to be suitable for  $S_8^{32}$  as well as for  $S_4N_4H_4^{32}$  and should therefore be applicable to  $S_7NH$  too. The details have been discussed in earlier papers.<sup>1-4,9,32</sup>

The following 16 independent force constants were used:

$K_1$	SS stretching
$K_2$	SN stretching
$K_3$	ND stretching
$H_1$	bending at S
$H_2$	SNS bending
$H_3$	SNH bending
$H_4$	NH wagging
$F_1$	SS repulsion
$F_2$	SN repulsion
$F_3$	SH repulsion
$Y_1$	SS torsion
$Y_2$	SN torsion
$C$	long-range SS and SN repulsion
$P_1$	bond-bond interaction at S
$P_2$	bond-bond interaction at N
$U$	NH wagging-SN torsion interaction

With these constants the potential energy becomes

$$\begin{aligned}
 2V = & \sum^6 K_1(\Delta r)^2 + 2\sum^6 K_1'r(\Delta r) + \sum^2 K_2(\Delta r)^2 \\
 & + 2\sum^2 K_2'r(\Delta r) + K_3(\Delta R)^2 + 2K_3'R(\Delta R) \\
 & + \sum^7 H_1(r\Delta\alpha)^2 + 2\sum^7 H_1'r(r\Delta\alpha) + H_2(r\Delta\alpha)^2 \\
 & + 2H_2'r(r\Delta\alpha) + \sum^2 H_3(\bar{r}\Delta\beta)^2 + 2\sum^2 H_3'\bar{r}(\bar{r}\Delta\beta) \\
 & + H_4(R\Delta\gamma)^2 + 2H_4'R(R\Delta\gamma) + \sum^6 F_1(\Delta q_1)^2 \\
 & + 2\sum^6 F_1'q_1(\Delta q_1) + \sum^2 F_2(\Delta q_2)^2 + 2\sum^2 F_2'q_2(\Delta q_2) \\
 & + \sum^2 F_3(\Delta q_3)^2 + 2\sum^2 F_3'q_3(\Delta q_3) + \sum^6 Y_1(r\Delta\tau)^2 \\
 & + 2\sum^6 Y_1'r(r\Delta\tau) + \sum^2 Y_2(r\Delta\tau)^2 + 2\sum^2 Y_2'r(r\Delta\tau) \\
 & + \sum^8 C(\Delta q')^2 + 2\sum^8 C'q'(\Delta q') + 2\sum^7 P_1\Delta r\Delta r' \\
 & + 2P_2\Delta r\Delta r' + 2\sum^2 U\Delta\gamma\Delta\tau
 \end{aligned}$$

The coordinates  $q$  and  $q'$  are the distances between atoms  $i$  and, respectively,  $i+2$  and  $i+3$ , and  $r$  and  $r'$  are the distances of adjacent bonds within the ring. Since all the distances  $q'$  are very similar ( $4.15 < q' < 4.45$  Å) only one force constant  $C$  was used.<sup>33</sup> Any long-range repulsion involving the hydrogen atom was neglected. The constants  $F'$  and  $C'$  were constrained by the conventional assumptions  $F' = -0.1F$  and  $C' = -0.1C$ . All constants  $K'$ ,  $H'$ , and  $Y'$  are eliminated in the removal of the redundant coordinates  $q$  and  $q'$ .

## Calculations

The calculations were performed by a CD 6500 computer using the programs UBZM by Schachtschneider<sup>34</sup> to calculate the  $Z$  matrix elements for the force constant  $C$  and BGLZ and LSMA by Shimanouchi<sup>35</sup> to calculate all matrices, the frequencies, and potential energy distribution. The valence force constants were obtained from the  $F$  matrix.

The Cartesian coordinates were taken from the recent low temperature x-ray structure analysis.<sup>13</sup> However, the NH bond length was assumed to be 1.03 Å which is the average in a large number of NH compounds and the hydrogen was assumed to be in the plane of the neigh-

boring atoms ( $\beta_1 = \beta_2 = 118.1^\circ$ ).<sup>36</sup> The symmetry coordinates with exception of the NH wagging coordinate  $S = \Delta\gamma$  were taken from  $S_8O_9$  ( $\gamma$  is the angle between the NH bond and the plane of atoms 6-8).

## Force Constants

The first set of frequencies was calculated with assumed Urey-Bradley force constants whose values were chosen using the force constants of  $S_8^{32}$  and  $S_4N_4H_4^{32}$ . To adjust the calculated to the observed frequencies by the least-squares method 38 observed values were used for  $S_7NH(\nu_2-\nu_4, \nu_7-\nu_{14}, \nu_{18}-\nu_{21})$ ,  $S_7ND(\nu_{1-21})$ ,  $S_7^{15}NH(\nu_{14})$ , and  $S_7^{15}ND(\nu_{14})$ .  $\nu_{NH}$  was neglected because of its anharmonicity. Solution frequencies were taken above  $750\text{ cm}^{-1}$ , otherwise solid state values were used.

First groups of force constants were varied but in the last run all 16 force constants were allowed to vary simultaneously until the corrections became zero. The frequencies obtained as well as the potential energy distribution are given in Table VI. The force constants are listed in Tables VII and VIII.

The maximum difference between observed and calculated wavenumbers amounts to  $9\text{ cm}^{-1}$ .

## Discussion

The Urey-Bradley and valence force constants of  $S_7NH$  can be compared with those of  $S_8^{32}$  and  $S_4N_4H_4^{32}$ . This comparison shows that all corresponding values are very similar indicating that the frequency assignment of  $S_7NH$  is correct and that the force field is appropriate. It should be pointed out, however, that the force constants connected with the wagging mode of  $S_7NH$  cannot be considered as reliable as those of  $S_4N_4H_4$  which exhibits three wagging modes from which the force constants can be determined more accurately. The normal-coordinate treatment of  $S_4N_4H_4$  has shown that in addition to the wagging-torsion interaction also wagging-stretching and wagging-bending interaction force constants are necessary which, however, could not be used in the case of  $S_7NH$  because of the only one wagging frequency. Nevertheless, all constants connected with the NH group are very similar in  $S_7NH$  and  $S_4N_4H_4$ .

There exist relationships between bond distances and  $SN^{39}$  and  $SS^5$  stretching force constants. The mean values calculated for  $S_7NH$  (Table VIII) are in agreement with these equations (calcd  $f_r(SN) = 3.9$ ,  $f_r(SS) = 2.47\text{ mdyn/Å}$ ). However, we have no explanation for the two different SS stretching force constants.

The average SS stretching frequency of  $S_7ND$  of  $453\text{ cm}^{-1}$  is in agreement with the value of  $458\text{ cm}^{-1}$  calculated from the bond distance-stretching frequency relationship.<sup>5</sup> The average SN stretching frequency of  $S_7NH$  ( $751\text{ cm}^{-1}$ ), however, does not fit the known bond distance-stretching frequency relationship<sup>40</sup> derived from only a few values some of which are not longer valid. Therefore, this relationship should be reinvestigated.

Nelson<sup>14</sup> observed a number of very weak Raman lines in the SN stretching region of  $S_7NH$  whose frequencies do not agree with the two infrared active  $\nu_{SN}$  modes. She explained these lines by factor group splitting of the  $\nu_{SN}$ . However, we did not observe these lines and the small frequency shift of the two  $\nu_{SN}$  modes on dissolution of  $S_7NH$  in  $CS_2$  does not support the idea of any measurable correlation field splitting. We therefore believe that the weak Raman lines are combination vibrations. We did also not observe the splitting of  $\delta_{SNH}(a'')$  reported by Nelson.

The most peculiar detail of the  $S_7NH$  spectrum is the NH wagging mode giving rise to three strong IR bands near

TABLE VI: Observed and Calculated Wavenumbers of  $S_7NH$  and  $S_7ND$  and Potential Energy Distribution to the Symmetry Coordinates<sup>a</sup>

$S_7^{14}NH$				$S_7^{14}ND$			
Wavenumber, $cm^{-1}$		Potential energy, (%)		Wavenumber, $cm^{-1}$		Potential energy, %	
Obsd	Calcd			Obsd	Calcd		
$a' \nu_1$	(3334)	3393	100 $\nu_{NH}$	2475	2475	99 $\nu_{ND}$	
$\nu_2$	694	693	83 $\nu_{SN}$ , 13 $\delta_{SNS}$	680	681	84 $\nu_{SN}$ , 12 $\delta_{SNS}$	
$\nu_3$	498	498	45 $\gamma$ , 44 $\nu_{SS}$	474	477	88 $\nu_{SS}$	
$\nu_4$	472	465	88 $\nu_{SS}$	463	461	85 $\nu_{SS}$ , 12 $\delta_{SSS}$	
$\nu_5$	(456)	450	93 $\nu_{SS}$	439	448	97 $\nu_{SS}$	
$\nu_6$	(433)	436	52 $\nu_{SS}$ , 38 $\gamma$	367	369	37 $\delta_{SSN}$ , 36 $\gamma$ , 12 $\nu_{SS}$	
$\nu_7$	356	357	60 $\delta_{SSN}$ , 12 $\tau_{SN}$ , 12 $\nu_{SS}$	327	327	56 $\delta_{SSN}$ , 20 $\tau_{SN}$ , 15 $\gamma$	
$\nu_8$	279	281	39 $\delta_{SNS}$ , 22 $\gamma$ , 13 $\tau_{SN}$ , 13 $\delta$	276	274	37 $\delta_{SNS}$ , 33 $\gamma$	
$\nu_9$	249	245	75 $\delta_{SSS}$	247	244	69 $\delta_{SSS}$ , 14 $\gamma$	
$\nu_{10}$	215	214	63 $\delta_{SSS}$ , 18 $\tau_{SS}$	214	213	61 $\delta_{SSS}$ , 14 $\tau_{SS}$	
$\nu_{11}$	160	162	77 $\delta_{SSS}$	159	161	75 $\delta_{SSS}$ , 11 $\gamma$	
$\nu_{12}$	71	70	39 $\gamma$ , 33 $\tau_{SN}$ , 21 $\tau_{SS}$	70	70	39 $\gamma$ , 33 $\tau_{SN}$ , 21 $\tau_{SS}$	
$a'' \nu_{13}$	1288	1290	98 $\delta_{NH}$	970	968	81 $\delta_{ND}$ , 19 $\nu_{SN}$	
$\nu_{14}$	805.8	808	98 $\nu_{SN}$	774.5	773	93 $\nu_{SN}$	
$\nu_{15}$	(472)	462	93 $\nu_{SS}$	463	462	93 $\nu_{SS}$	
$\nu_{16}$	(456)	459	87 $\nu_{SS}$	455	459	87 $\nu_{SS}$	
$\nu_{17}$	(427)	423	99 $\nu_{SS}$	428	423	99 $\nu_{SS}$	
$\nu_{18}$	261	256	59 $\delta_{SSN}$ , 28 $\delta_{SSS}$	262	255	58 $\delta_{SSN}$ , 29 $\delta_{SSS}$	
$\nu_{19}$	212	214	58 $\delta_{SSS}$ , 18 $\tau_{SS}$	211	213	57 $\delta_{SSS}$ , 22 $\tau_{SS}$	
$\nu_{20}$	160	168	70 $\delta_{SSS}$ , 23 $\delta_{SSN}$	159	168	70 $\delta_{SSS}$ , 23 $\delta_{SSN}$	
$\nu_{21}$	91	92	65 $\tau_{SS}$ , 26 $\tau_{SN}$	91	92	64 $\tau_{SS}$ , 25 $\tau_{SN}$	

 $S_7^{15}NH$ :  $\nu_{SN}(a'')$  obsd 787.0, calcd 788 $S_7^{15}ND$ :  $\nu_{SN}(a'')$  obsd 762.0, calcd 760<sup>a</sup>  $\geq 10\%$ ; wavenumbers in brackets were not used in the force constant calculation.

TABLE VII: Urey-Bradley Force Constants of Heptasulfur Imide (mdyn/Å)

$K_1(SS)$	1.751	$H_4(NH)$	0.180	$Y(SS)$	0.023
$K_2(SN)$	2.805	$F_1(SS)$	0.347	$Y(SN)$	0.045
$K_3(ND)$	5.749	$F_2(SN)$	0.703	$C$	0.039
$H_1(S)$	0.053	$F_3(SH)$	0.552	$U(\gamma/\tau)$	0.142
$H_2(SNS)$	0.199	$P_1(S)$	0.236		
$H_3(SNH)$	0.109	$P_2(N)$	0.572		

TABLE VIII: Valence Force Constants of Heptasulfur Imide (mdyn/Å)<sup>a</sup>

$f_r(SS)$	2.23 ( $r_1 - r_4$ )	$f_a$	0.23 ( $a_1 - a_5$ )
$f_r(SN)$	2.53 ( $r_5, r_6$ )	$f_a$	0.36 ( $a_6, a_7$ )
$f_r(ND)$	3.98	$f_a$	0.33 ( $a_8$ )
$f_{rr}(SS/SS)$	6.37	$f_\beta$	0.28
$f_{rr}(SS/SN)$	0.52	$f_\gamma$	0.18
$f_{rr}(SN/SN)$	0.80	$f_\tau$	0.03 (SSSS)
$f_{rr}(SN/ND)$	0.90	$f_\tau$	0.04 (SSSN)
$f_{rr}(SN/NH)$	0.41	$f_\tau$	0.05 (SSNS)
$f_{ra}$	0.15-0.31	$f_{\gamma\tau}$	0.14
$f_{r\beta}(SN/NH)$	0.31		

<sup>a</sup>  $f_i$ , diagonal constants;  $f_{ij}$ , interaction constants between the nearest coordinates indicated.

450  $cm^{-1}$ . The potential energy distribution shows  $\gamma_{NH}$  to be mixed with many other  $a'$  vibrations but this result may be partly unreal since the PED with respect to  $\gamma_{NH}$  was quite sensitive to the kind and the values of certain force constants (94 different sets of force constants were examined). We, therefore, doubt that the three IR bands at 427, 456, and 500  $cm^{-1}$  arise all from coupling of  $\gamma_{NH}$  with two or three SS stretching vibrations. Only the highest band at 500  $cm^{-1}$  is believed to be a mixture of  $\gamma_{NH}$  and  $\nu_{SS}$ . The remaining "doublet" at 427/456  $cm^{-1}$  must be caused by a double minimum potential as discussed above or by Fermi resonance of  $\gamma_{NH} \approx 450$   $cm^{-1}$  with a combination vibration. There are indeed several suitable binary combinations belonging to the  $a'$  species (for example, 2-214, 2-212, 356 + 71, 279 + 160). However, there are also combinations close to  $\gamma_{ND} = 367$   $cm^{-1}$  but no Fermi resonance is observed. We therefore favor the explanation

by a double minimum potential.

**Acknowledgment.** The author is grateful to Miss B. Pawlaczyk for her assistance in preparing heptasulfur imide and to Dipl.-Chem. F. Rose for running the low temperature spectra. The financial support by the Bundesminister für Wirtschaft (ERP-Sondervermögen) and the Verband der Chemischen Industrie is also gratefully acknowledged.

## References and Notes

- (1) L. A. Nimmon and V. D. Neff, *J. Mol. Spectrosc.*, **26**, 175 (1968).
- (2) D. W. Scott, J. P. McCullough, and F. H. Kruse, *J. Mol. Spectrosc.*, **13**, 313 (1964).
- (3) R. Steudel and D. F. Eggers, *Spectrochim. Acta, Part A*, **31**, 879 (1975).
- (4) R. Steudel, *Spectrochim. Acta, Part A*, **31**, 1065 (1975).
- (5) R. Steudel, *Z. Naturforsch. B*, **30**, 281 (1975).
- (6) R. Steudel and J. Latte, *Angew. Chem.*, **86**, 648 (1974).
- (7) P. Luger, H. Bradaczek, R. Steudel, and M. Rebsch, *Chem. Ber.*, **109**, 180 (1976).
- (8) R. Steudel and M. Rebsch, *J. Mol. Spectrosc.*, **51**, 334 (1974).
- (9) R. Steudel and D. F. Eggers, *Spectrochim. Acta, Part A*, **31**, 871 (1975).
- (10) J. Bojes and T. Chivers, *J. Chem. Soc., Dalton Trans.*, 1715 (1975).
- (11) J. Weiss, *Z. Anorg. Allg. Chem.*, **305**, 191 (1960).
- (12) J. Weiss and H.-S. Neubert, *Acta Crystallogr.*, **18**, 815 (1965).
- (13) H. J. Hecht, R. Reinhardt, R. Steudel, and H. Bradaczek, *Z. Anorg. Allg. Chem.*, **426**, 43 (1976).
- (14) J. Nelson, *Spectrochim. Acta, Part A*, **27**, 1105 (1971).
- (15) E. R. Cole and R. F. Bayfield in A. Senning, "Sulfur in Organic and Inorganic Chemistry", Vol. 2, Marcel Dekker, New York, N.Y., 1972, p 223.
- (16) T. Chivers and I. Drummond, *Inorg. Chem.*, **13**, 1222 (1974).
- (17) R. Steudel, *Z. Anorg. Allg. Chem.*, **360**, 143 (1968).
- (18) D. J. Gardiner, *J. Mol. Spectrosc.*, **38**, 476 (1971).
- (19) C. D. Bass, L. Lynds, T. Wolfram, and E. E. DeWames, *J. Chem. Phys.*, **40**, 3611 (1964).
- (20) G. E. Moore and R. M. Badger, *J. Am. Chem. Soc.*, **74**, 6076 (1952).
- (21) R. Steudel and F. Rose, unpublished results.
- (22) E. M. Tingle and F. P. Olsen, *Inorg. Chem.*, **8**, 1741 (1969).
- (23) R. Clements, R. L. Dean, T. R. Singh, and J. L. Wood, *Chem. Commun.*, 1125, 1127 (1971).
- (24) R. L. Somorjai and D. F. Hornig, *J. Chem. Phys.*, **36**, 1980 (1962).
- (25) J. L. Wood, *J. Mol. Struct.*, **12**, 283 (1972).
- (26) R. Steudel, F. Rose, and J. Pickardt, *Z. Anorg. Allg. Chem.*, in press.
- (27) The bending mode of the triatomic molecule  $S_2O$  occurs at 382  $cm^{-1}$ .<sup>28</sup>
- (28) A. G. Hopkins, F. P. Daly, and C. W. Brown, *J. Phys. Chem.*, **79**, 1849 (1975).
- (29) R. Steudel and F. Rose, *Z. Naturforsch. B*, **30**, 810 (1975).
- (30) A. T. Ward, *J. Phys. Chem.*, **72**, 744 (1968).

- (31) G. A. Ozin, *J. Chem. Soc. A*, 116 (1969).  
 (32) R. Steudel and F. Rose, *Spectrochim. Acta*, submitted for publication.  
 (33) The correlation of Urey-Bradley force constants with structural parameters of sulfur rings has been discussed in ref 4.  
 (34) J. H. Schachtschneider, "Vibrational Analysis of Polyatomic Molecules V", Reprint no. 231-64, Emeryville, Calif.  
 (35) T. Shimanouchi, Computer Programs for Normal Coordinate Treatment of Polyatomic Molecules, Tokyo, 1968.  
 (36) See the structures of  $S_2N_4H_4^{37}$  and of  $(SNCH_3)_4^{38}$  the geometry at the nitrogens of these molecules is planar or quasiplanar.  
 (37) T. M. Sabine and G. W. Cox, *Acta Crystallogr.*, **23**, 574 (1967).  
 (38) A. L. MacDonald and J. Trotter, *Can. J. Chem.*, **51**, 2504 (1973).  
 (39) O. Glemser, A. Muller, D. Bohler, and B. Krebs, *Z. Anorg. Allg. Chem.*, **357**, 184 (1966).  
 (40) A. J. Banister, L. F. Moore, and J. S. Padley, *Spectrochim. Acta, Part A*, **23**, 2705 (1967).

## A Detailed Study of *N,N,N',N'*-Tetramethyl-*p*-phenylenediamine Luminescence in Organic Glasses. Evidence for a Protonation Reaction

J. Blais and M. Gauthier\*

E.R. CNRS 98, Laboratoire de Chimie Physique Bât. 350, Université Paris-Sud 91405, Orsay, France (Received February 22, 1976; Revised Manuscript Received November 8, 1976)

Publication costs assisted by CNRS

The solvent and temperature dependence of an anomalous long-lived luminescence ( $\lambda_{\max}$  430 nm), observed simultaneously with the ordinary fluorescence and phosphorescence of tetramethyl-*p*-phenylenediamine (TMPD) in ethanol and in some other organic solvents at 77 K, has been studied. These results together with some complementary observations on absorption spectra have been interpreted as indicative of a protonation by ethanol of the TMPD molecule in its ground state. It is also shown that when excited to the first singlet,  $TMPDH^+$  is partially decomposed to  $TMPD^S$ , the spectral properties of which are different from that of the directly excited TMPD. The mechanism of protonation and the importance of the environment on spin-orbit coupling of TMPD are discussed.

### Introduction

Aromatic amines in organic glasses have been the subject of several luminescence studies in the last decade.<sup>1-3</sup> Among them, *N,N,N',N'*-tetramethyl-*p*-phenylenediamine (TMPD) is of particular interest. Due to its low ionization potential, it is the most commonly used solute for photoionization studies in liquid or glassy solutions. Its UV excited luminescence<sup>4</sup> as well as the neutralization luminescence following photoionization<sup>5</sup> have been extensively studied. In a previous paper,<sup>6</sup> we reported the existence of a new type of long-lived luminescence characterized by excitation and emission spectra which appear quite distinct from the TMPD absorption and emission. The species responsible for this emission was tentatively identified with a solute-solvent charge transfer state, the existence of which had been repeatedly postulated in glasses<sup>7</sup> as well as in liquids<sup>8</sup> to account for some anomalies noted in photoionization studies.

Further experimental results do not support this early interpretation and the experimental evidence given below shows that the luminescence is associated with the protonated form  $TMPDH^+$ . Moreover, it has been observed that upon excitation  $TMPDH^+$  is partly decomposed to  $TMPD^*$  and that the luminescent properties of the latter are somewhat different from those of the directly excited TMPD molecule.

### Experimental Section

**Reagents.** TMPD was liberated from the hydrochloride salt with NaOH and purified by several sublimations just before use. Methylcyclohexane (Eastman Kodak spectrograde) and 3-methylpentane (Koch Light) were purified by chromatography on activated silica gel and alumina ("standard" MCH and 3MP). Ethanol (Merck) was distilled on acid 2,4-dinitrophenylhydrazine and dried over  $I_2$ -Mg in accord with the Lund and Bjerrum method

("standard" ethanol). Triethylamine (TEA, Fluka) was distilled over potassium hydroxide. The solvents were purified just before use and their purity was tested by absorption and emission spectroscopy. The classical methods of purification described above have been used in most experiments. However, for solvents denoted below as "dry" further dehydration was performed by keeping the solvent several hours on a sodium mirror (for MCH and TEA), on anhydrous  $CaSO_4$  (for ethanol), or on molecular sieves (for MCH, ethanol, 2,2,2-trifluoroethanol (Fluka), acetonitrile (uvasol Merck)). In all cases, the treatment was done under vacuum and the solutions were prepared by dilution in the same vacuum system after distillation of the solvent. The samples were finally sealed in a nonfluorescent silica tube (3 mm i.d.) for low temperature measurements or in a 10-mm square silica cell for room temperature experiments.

**Apparatus and Measurements.** The absorption spectra were obtained with a Zeiss PMQ II spectrophotometer equipped to make low temperature measurements.<sup>9</sup> The luminescence spectra were recorded with a Jobin-Yvon "Bearn" spectrofluorimeter equipped with a phosphoroscope. The spectral bandwidth was 3-6 nm for excitation and 6-12 nm for analysis. The relative emission intensities were obtained from areas measured on intensity vs. wavenumber curves. It has been determined that the intensity vs. wavelength dependence of the analyzing monochromator and photomultiplier system is constant to within 10% in the 350-510-nm spectral range. An abrupt decrease of sensitivity only occurs for wavelengths longer than 550 nm. Thus the intensity data were determined from the observed uncorrected emission spectra. The observed excitation spectra were corrected to a constant number of photons in the exciting beam. The spectral composition of the exciting light was itself obtained by the use of rhodamine B as a quantum counter.